TRANSFER ORBITS IN THE EARTH – MOON SYSTEM AND REFINEMENT TO JPL EPHEMERIDES

Elisa Maria Alessi[(1)], **Gerard Gómez**[(1)], **Josep J. Masdemont**[(2)]

[(1)] *IEEC & Dpt. Matemàtica Aplicada i Anàlisi, Universitat de Barcelona, Gran Via 585, 08007 Barcelona, Spain.*
E-mail: elim@maia.ub.es, gerard@maia.ub.es
[(2)] *IEEC & Dpt. Matemàtica Aplicada I, Universitat Politècnica de Catalunya, Diagonal 647, 08028 Barcelona, Spain.*
E-mail: josep@barquins.upc.edu

Abstract

We describe how to determine transfers between libration point orbits and either the surface of the Moon or a Low Earth Orbit within the Circular Restricted Three – Body Problem (CR3BP) assumptions. Moreover, we explain how to refine such trajectories to ones verifing more comprehensive equations of motion. We are interested in seeing how the geometry of the nominal target orbits and of the associated stable manifolds drives the connections and also how much reliable the CR3BP is. The main tools we take advantage of are the Lindstedt–Poincaré semi-analytical method, differential correction procedures and an optimizer.

1 INTRODUCTION

The main purpose of this work is to compute trajectories that can connect a nominal libration point orbit (LPO) either with the surface of the Moon or with a given Low Earth Orbit (LEO). The motivation of this arises from the new effort that worldwide space agencies are devoting to the lunar exploration.

In a first step, we consider as force field model the Circular Restricted Three – Body Problem (CR3BP) and we focus on periodic and quasi-periodic orbits either around the point L_1 or the point L_2.

We construct lunar rescue orbits, by exploiting the stable invariant manifolds associated with halo and Lissajous orbits around a nominal equilibrium point. We are interested in ascertaining from which lunar regions the transfers can be achieved, the minimum departing velocity required, the time of flight and the departure angle, dedicating particular attention to orthogonal takeoff.

With respect to the transfers from a well-defined LEO to a certain Lissajous orbit, it is not sufficient to take advantage of the corresponding stable manifold, because it does not reach the Earth. We need an additional transfer leg. In this case, the main interest resides in seeing how the transfer's total cost and time depend on the geometry of the arrival orbit and on the points at which the manoeuvres are performed.

In a further step, we consider the spacecraft to be affected by the Sun, the Moon and the nine planets, whose position and velocity are provided by the JPL ephemerides. We define a constrained optimisation problem, by considering as objective function one which accounts for the total Δv – cost along the path and asking the solution to fulfill some specific requirements in terms of position and time. Roughly speaking, we would like to understand how a nominal trajectory obtained via a simplified model of forces can be translated into a different vectorfield. At this stage, our aim is to see how much accurate the results obtained by applying the CR3BP are, but also to produce a powerful tool that can be employed in other situations.

2 THE MODELS

In what follows, we work with two different vectorfields, both of them considering only gravitational attractions as main forces acting on the probe. In the Circular Restricted Three – Body Problem approximation, the Earth and the Moon affect the motion of the spacecraft; in the Restricted N – Body Problem (RNBP) assumptions, the Sun, the Moon and the nine planets are present.

2.1 The Circular Restricted Three – Body Problem

The Circular Restricted Three – Body Problem [1] studies the behaviour of a particle P with infinitesimal mass m_3 moving under the gravitational attraction of two primaries P_1 and P_2, of masses m_1 and m_2, revolving around their center of mass in circular orbits.

To remove time from the equations of motion, it is convenient to introduce a synodical reference system $\{O, x, y, z\}$, which rotates around the z–axis with a constant angular velocity ω equal to the mean motion n of the primaries. The origin of the reference frame is set at the barycenter of the system and the x–axis on the line which joins the primaries, oriented in the direction of the largest primary. In this way we work with m_1 and m_2 fixed on the x–axis.

The units are chosen in such a way that the distance between the primaries and the modulus of the angular velocity of the rotating frame are unitary. We define the mass ratio μ as $\mu = \frac{m_2}{m_1+m_2}$. For the Earth – Moon system, the unit of distance equals 384400 km, the unit of velocity equals 1.02316 km/s and the dimensionless mass of the Moon is $\mu = 0.012150582$.

The equations of motion can be written as

$$\begin{aligned} \ddot{x} - 2\dot{y} &= x - \frac{(1-\mu)}{r_1^3}(x-\mu) - \frac{\mu}{r_2^3}(x+1-\mu), \\ \ddot{y} + 2\dot{x} &= y - \frac{(1-\mu)}{r_1^3}y - \frac{\mu}{r_2^3}y, \\ \ddot{z} &= -\frac{(1-\mu)}{r_1^3}z - \frac{\mu}{r_2^3}z, \end{aligned} \tag{1}$$

where $r_1 = [(x-\mu)^2 + y^2 + z^2]^{\frac{1}{2}}$ and $r_2 = [(x+1-\mu)^2 + y^2 + z^2]^{\frac{1}{2}}$ are the distances from P to P_1 and P_2, respectively.

The system (1) has a first integral, the Jacobi integral, which is given by

$$C = x^2 + y^2 + \frac{2(1-\mu)}{r_1} + \frac{2\mu}{r_2} + (1-\mu)\mu - \left(\dot{x}^2 + \dot{y}^2 + \dot{z}^2\right). \tag{2}$$

In the synodical reference system, there exist five equilibrium (or libration) points. Three of them, the collinear ones, are in the line joining the primaries and are usually denoted by L_1, L_2 and L_3. If x_{L_i} ($i = 1, 2, 3$) denotes the abscissa of the three collinear points, we assume that

$$x_{L_2} < \mu - 1 < x_{L_1} < \mu < x_{L_3}.$$

The collinear libration points behave as the product of two centers by a saddle. When we consider all the energy levels, the center $\times$ center part gives rise to 4–dimensional central manifolds around these equilibria.

Among the solutions filling the central invariant manifolds, the quasi-periodic Lissajous orbits are associated with two–dimensional tori, whose two basic frequencies ω and ν tend, respectively, to the frequencies related to both centers, ω_p and ω_v, when the amplitudes tend to zero. They are characterized by an harmonic motion in the $\{z = 0\}$ plane (the in-plane component) and an uncoupled oscillation in z–direction (the out-of-plane component) with different periods. The halo orbits are three-dimensional periodic orbits symmetric with respect to the $\{y = 0\}$ plane. In this case, the in-plane motion and the out-of-plane one have the same period.

Due to the hyperbolic character, the dynamics close to the collinear libration points is that of an unstable equilibrium. This means that each type of central orbits around L_1, L_2 and L_3 has a stable and an unstable invariant manifold. They look like tubes of asymptotic trajectories tending to, or departing from, the corresponding orbit. These tubes have a key role in the study of the natural dynamics of the libration regions. When going forwards in time, the trajectories on the stable manifold approach exponentially the orbit, while those on the unstable manifold depart exponentially. Each manifold has two branches, a positive and a negative one.

2.1.1 Computation of central and hyperbolic invariant manifolds

The computation of the central and the hyperbolic objects can be done in different ways. We use a Lindstedt–Poincaré procedure, which determines semi-analytical expressions for the invariant objects in terms of suitable amplitudes and phases by series expansions [2]. The approach is semi-analytical in the sense that we compute the numerical values of the coefficients of the series.

Let us set the origin of the coordinates at the libration point and scale the variables in such a way that the distance from the smallest primary to the chosen equilibrium point will be equal to one [3]. In this reference system the CR3BP equations of motions are

$$\begin{aligned} \ddot{x} - 2\dot{y} - (1 + 2c_2)x &= \frac{\partial}{\partial x} \sum_{n \geq 3} c_n \rho^n P_n\Big(\frac{x}{\rho}\Big), \\ \ddot{y} + 2\dot{x} + (c_2 - 1)y &= \frac{\partial}{\partial y} \sum_{n \geq 3} c_n \rho^n P_n\Big(\frac{x}{\rho}\Big), \\ \ddot{z} + c_2 z &= \frac{\partial}{\partial z} \sum_{n \geq 3} c_n \rho^n P_n\Big(\frac{x}{\rho}\Big), \end{aligned} \tag{3}$$

where $\rho^2 = x^2 + y^2 + z^2$, P_n is the Legendre polynomial of order n and the c_n are suitable constants that only depend on the libration point and on μ.

The formal series solution is of the type

$$\begin{aligned} x(t) &= \sum \exp(i-j)\theta_3[x^{pq}_{ijkm}\cos(p\theta_1+q\theta_2)+\bar{x}^{pq}_{ijkm}\sin(p\theta_1+q\theta_2)]\alpha_1^i\alpha_2^j\alpha_3^k\alpha_4^m, \\ y(t) &= \sum \exp(i-j)\theta_3[y^{pq}_{ijkm}\cos(p\theta_1+q\theta_2)+\bar{y}^{pq}_{ijkm}\sin(p\theta_1+q\theta_2)]\alpha_1^i\alpha_2^j\alpha_3^k\alpha_4^m, \\ z(t) &= \sum \exp(i-j)\theta_3[z^{pq}_{ijkm}\cos(p\theta_1+q\theta_2)+\bar{z}^{pq}_{ijkm}\sin(p\theta_1+q\theta_2)]\alpha_1^i\alpha_2^j\alpha_3^k\alpha_4^m, \end{aligned} \tag{4}$$

where $\theta_1 = \omega t + \phi_1$, $\theta_2 = \nu t + \phi_2$ and $\theta_3 = \lambda t$, $\omega = \sum \omega_{ijkm}\alpha_1^i\alpha_2^j\alpha_3^k\alpha_4^m$, $\nu = \sum \nu_{ijkm}\alpha_1^i\alpha_2^j\alpha_3^k\alpha_4^m$, $\lambda = \sum \lambda_{ijkm}\alpha_1^i\alpha_2^j\alpha_3^k\alpha_4^m$ and summations are extended over all $i, j, k, m \in \mathbb{N}$ and $p, q \in \mathbb{Z}$.

The Lindstedt–Poincaré procedure computes the coefficients x^{pq}_{ijkm}, y^{pq}_{ijkm}, z^{pq}_{ijkm}, ω_{ijkm}, ν_{ijkm} and λ_{ijkm} up to a finite order N.

In this way, for a given equilibrium point and for a certain epoch t, we can compute the position and the velocity of the particle in terms of the four amplitudes α_1, α_2, α_3, α_4 and the two phases ϕ_1, ϕ_2. Setting $\alpha_1 = \alpha_2 = 0$ we obtain Lissajous orbits of amplitudes α_3 and α_4 and phases ϕ_1 and ϕ_2; setting $\alpha_1 = 0$, but $\alpha_2 \neq 0$ ($\alpha_2 = 0$, $\alpha_1 \neq 0$) we get the stable (unstable) manifold.

Halo orbits appear when the two frequencies ω and ν are equal. In this case, we look for expansions of the solution analogous to (4), adding a Δz term to the third differential equation in (3) and imposing

$$\Delta = \sum \Delta_{ijkm}\alpha_1^i\alpha_2^j\alpha_3^k\alpha_4^m = 0. \tag{5}$$

As a consequence, the in-plane and out-of-plane amplitudes α_3 and α_4 are no longer independent. In the halo case just by fixing the value of α_4 we determine the size of the orbit and the value of α_3 is given straightforwardly. In the Lissajous case, we must give a value for both of them.

2.2 The Restricted N – Body Problem

In the Restricted N – body framework, we assume the massless particle to move under the gravitational influence of the Sun, the Moon and the nine planets. The conventional formulation considers an equatorial reference system centered at the Solar System barycenter with physical units of distance, time and mass (AU, day and kg). In this work, the position and velocity for the massive bodies, say $\mathbf{X}_p \equiv (x_p, y_p, z_p, \dot{x}_p, \dot{y}_p, \dot{z}_p)$, at a given instant of time are furnished by the JPL ephemerides DE405. The equations of motion for the spacecraft can be written as

$$\begin{aligned} \ddot{x} &= -\sum_{p=1}^{11} Gm_p\frac{(x-x_p)}{r_p^3}, \\ \ddot{y} &= -\sum_{p=1}^{11} Gm_p\frac{(y-y_p)}{r_p^3}, \\ \ddot{z} &= -\sum_{p=1}^{11} Gm_p\frac{(z-z_p)}{r_p^3}, \end{aligned} \tag{6}$$

where $r_p = \sqrt{(x-x_p)^2+(y-y_p)^2+(z-z_p)^2}$ is the distance between the planet p and the particle, G is the gravitational constant and m_p is the mass of the body p.

Since we are going to study the behaviour of a probe in the Earth – Moon neighbourhood, it is convenient to take into account its position and velocity with respect to the Earth. In other words, we

attempt to avoid the cancellation problems which might occur when considering a trajectory far from the Solar System barycenter. To this end, we perform the following change of coordinates:

$$\mathbf{\Xi} := \mathbf{X} - \mathbf{X}_E \equiv (x - x_E, y - y_E, z - z_E, \dot{x} - \dot{x}_E, \dot{y} - \dot{y}_E, \dot{z} - \dot{z}_E) =: (\xi, \eta, \zeta, \dot{\xi}, \dot{\eta}, \dot{\zeta}), \qquad (7)$$

where $\mathbf{X}_E$ represents position and velocity of the Earth. The vectorfield to consider is now

$$\begin{aligned} \ddot{\xi} &= -\sum_{p=1}^{11} Gm_p \frac{(x_E - x_p + \xi)}{r_{Ep}^3} - \ddot{x}_E, \\ \ddot{\eta} &= -\sum_{p=1}^{11} Gm_p \frac{(y_E - y_p + \eta)}{r_{Ep}^3} - \ddot{y}_E, \\ \ddot{\zeta} &= -\sum_{p=1}^{11} Gm_p \frac{(z_E - z_p + \zeta)}{r_{Ep}^3} - \ddot{z}_E, \end{aligned} \qquad (8)$$

where $r_{Ep} = \sqrt{(x_E - x_p + \xi)^2 + (y_E - y_p + \eta)^2 + (z_E - z_p + \zeta)^2}$.

3 LPO – PRIMARY TRANSFERS

In this section, we explain the methodologies chosen in order to compute LPO – Moon and LPO – LEO transfers. Here we work under the CR3BP hypotheses. Halo and Lissajous orbits are computed with the Lindstedt–Poincaré procedure, the range of amplitudes explored following the numerical convergence domain of the series expansions, see [4] and [5].

3.1 Lunar Rescue Orbits

As lunar rescue orbits, we mean trajectories that allow to depart from the surface of the Moon having as target a LPO. In the CR3BP framework, these transfers lay on the stable invariant manifold associated with the nominal arrival orbit. We consider halo and Lissajous families either around the point L_1 or the point L_2 in the Earth – Moon system.

The approach adopted consists in the numerical globalisation of the stable manifold associated with the nominal LPO until it gets to the Moon backwards in time. The Moon is considered as a sphere of radius 1737.53 km. The initial conditions are computed by means of order 25 Lindstedt–Poincaré expansions setting $\alpha_1 = 0$ and $\alpha_2 \neq 0$ and taking a well-defined number of equally spaced values for ϕ_1 (and ϕ_2 in the Lissajous case) in $[0, 2\pi]$. The branch that gets close to the Moon is the positive one for the orbits around L_1 and the negative branch for L_2.

We recall that a stable invariant manifold is established on asymptotic trajectories. This means that to go from the Moon to a nominal LPO on such trajectories would take, in principle, an infinite time. Concretely, we start the numerical integration (i.e. we set $t = 0$) when we are at about 70 – 90 km from the reference arrival orbit.

Not all the orbits of a certain manifold can reach the surface of the Moon. Later on, we will see that it depends on the size of the arrival orbit considered and on the phase/phases associated with the trajectory of the invariant manifold. To prevent for long time integrations we set some controls. First, we set for each trajectory explored 10 adimensional time units (about 43.5 days) as maximum allowed

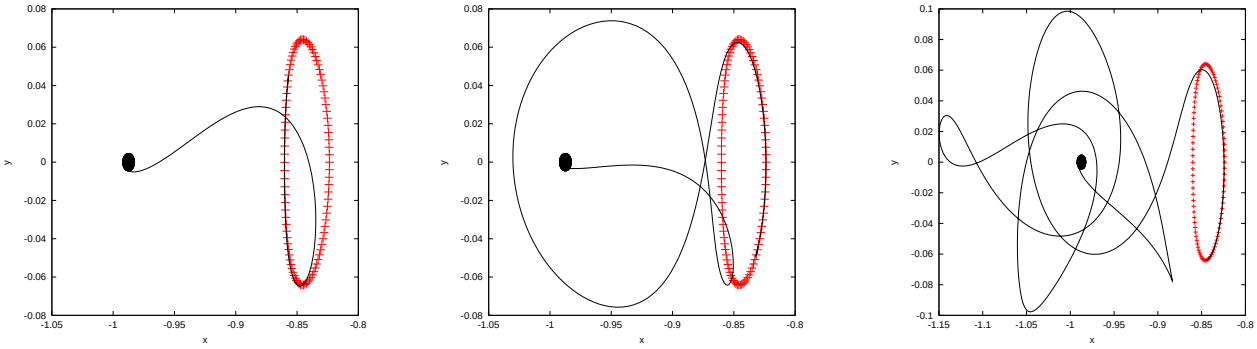

Figure 1: (x, y) projection of three trajectories of the stable invariant manifold associated with the halo orbit (in red) around the L_1 point of the Earth – Moon system with $\alpha_4 = 0.2$ normalized units (≈ 11000 km).

time. Increasing the final time, we would get some more collision orbits but, from a qualitative point of view, the results are almost identical.

The second control takes into account how many times the orbit has gone close to the Moon without getting to it. We are interested in almost direct transfers and we do not see operational advantages in trajectories winding around the Moon indefinitely.

If an orbit reaches the Moon's surface, we compute the latitude φ and the longitude λ corresponding to the arrival point, namely,

$$\varphi \;=\; \tan^{-1}\left(\frac{z}{\sqrt{(x-\mu+1)^2+y^2}}\right), \qquad \lambda \;=\; \tan^{-1}\left(\frac{y}{x-\mu+1}\right). \tag{9}$$

In our exploration $(\varphi = 0^\circ, \lambda = 0^\circ)$ corresponds to the Moon's point which is the closest to the Earth.

In addition, we calculate the physical velocity of arrival, the physical transfer time and the arrival angle ϑ, defined as the angle between the velocity vector and the Moon's surface normal vector.

In Fig. 1 we display three examples of the transfers computed. The target is the L_1 halo orbit with z–amplitude $\alpha_4 = 0.2$ normalized units (≈ 11000 km). The trajectory on the left reaches the Moon directly, the one in the middle performing one loop around the Moon and the one on the right performing four.

For halo orbits, the hyperbolic invariant manifolds are two-dimensional and their intersection with the Moon's surface is a curve. On the other hand, the hyperbolic invariant manifolds associated with Lissajous orbits are three-dimensional and hence we obtain two-dimensional regions on the Moon. In particular, if we fix one of the phases, say ϕ_1, and allow the other one to vary within $[0, 2\pi]$, the intersection with the surface of the Moon is a curve, which is closed if any value of ϕ_2 gives rise to an orbit which intersects the Moon's surface. As we change the value of ϕ_1, the intersection curve changes both in shape and position in the (λ, φ) plane. Of course, it might happen that for certain intervals of values of any of the phases, the intersection disappears.

The outcome reveals that we cannot reach a halo orbit, either around L_1 or L_2, with a rescue orbit leaving from an arbitrary point of the surface of the Moon without performing at least one loop around it. As we increase the number of loops, the area of the rescue region on the Moon increases. In fact, if we allow at least 3 loops, one can reach the halo families departing from any point.

However, we remark that the points of allowed departure are not uniformly distributed on the Moon's surface. There exist regions where we have more chances to take off joining the invariant manifold

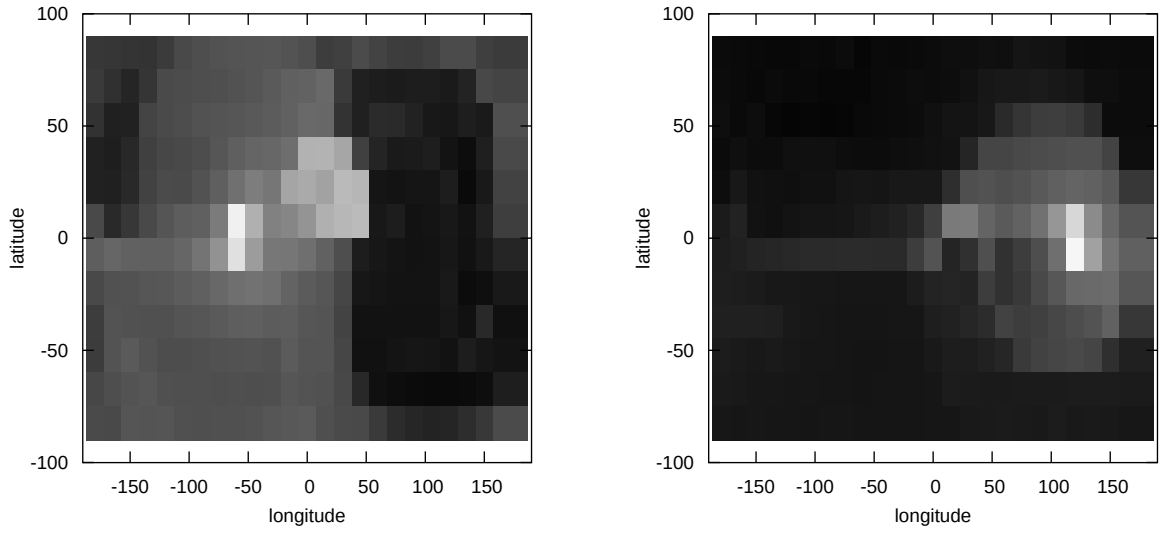

Figure 2: Number of opportunities of departure from the Moon's surface per unit of length of the halo arrival orbit and per unit of area element. A lighter color corresponds to a greater chance. On the left, the L_1 case; on the right, the L_2 one.

associated with a given halo orbit. In Fig. 2, we depict the density of opportunity of rescue, that is, the number of departures from the Moon per unit of length of the halo arrival orbit and per unit of area on the surface of the Moon. A lighter color corresponds to a greater probability of departure.

Regarding the Lissajous reference orbits, the most of the rescue orbits can reach them in a direct way if the Lissajous is around L_1, but the L_2 transfers need at least two loops around the Moon. In both cases, we are allowed to depart only from a lunar equatorial strip about 40° wide in terms of latitude.

Also, from our simulation it turns out that the stable manifolds intersect the Moon only if the ampli-

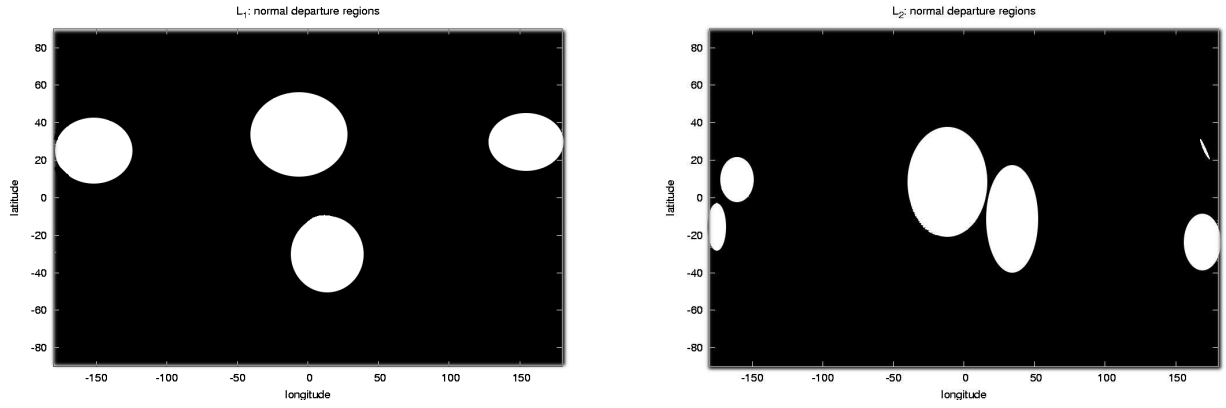

Figure 3: Regions of normal departure (the white ones) from the Moon to the halo family around L_1 (left) and L_2 (right). The two plots correspond to trajectories performing up to 3 loops around the Moon before reaching the halo orbit.

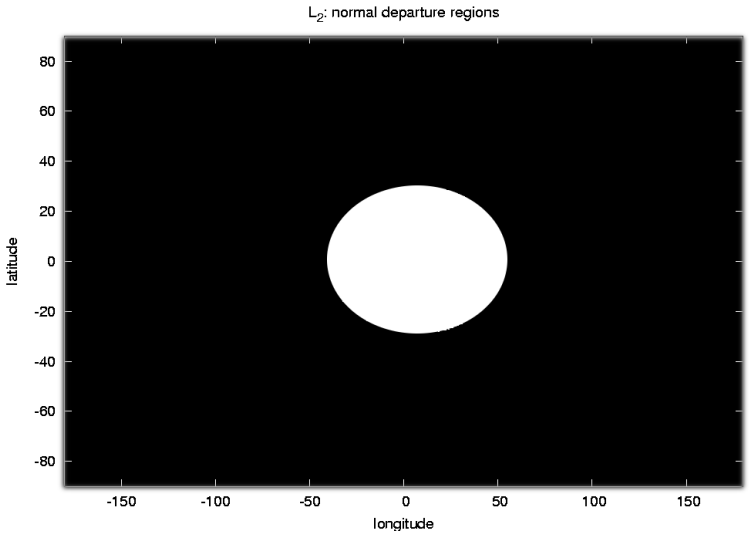

Figure 4: Region of normal departure (the white one) from the Moon to square ($\alpha_3 = \alpha_4$) Lissajous orbits around L_2. The plot corresponds to trajectories performing up to 5 loops around the Moon before reaching the quasi-periodic orbit.

tudes $\alpha_3 = \alpha_4$ are big enough, this is: $\alpha_3 = \alpha_4 > 0.064$ (≈ 4000 km) for L_1 and $\alpha_3 = \alpha_4 > 0.075$ (≈ 5000 km) for L_2.

Concerning the velocity of departure, we note that in all the cases it is almost equal to the escape velocity of the Moon (≈ 2.3 km/s). This is expected from the conservation of the Jacobi integral. The transfer time for all the direct transfers obtained is approximately 10 days. Each further loop takes about 10 more days.

In Fig. 3, we display the regions from which we can leave with an angle less than 10° and get to a halo orbit. No regions of orthogonal departure exist for L_1 Lissajous lunar rescue trajectories, while for the L_2 ones the departure region characterized by an angle less than 10° is shown in Fig. 4.

For the halo targets, there is a very large range of ϕ_1 (more than one half of the full range) which is not reached by the rescue orbits. For the quasi-periodic orbits we explored, the greater the amplitude of the Lissajous the greater the interval of values of ϕ_1 that give rise to rescue orbits.

More details can be found in [5].

3.2 LEO – Lissajous Transfers

As mentioned before, to move from a LEO to a LPO in the Earth – Moon system, the stable invariant manifold is not longer enough. The transfer is achieved by exploiting an additional trajectory, which is necessary to go from the nominal LEO to the reference stable manifold. In this part of the work, we take as target locations Lissajous orbits either around the point L_1 or the point L_2. The case of halo orbits has already been analyzed, for instance in [6], [7] and [8].

In the strategy adopted, we deal with a two–manoeuvres transfer. We leave from a nominal Lissajous orbit backwards in time on one of the branches of the corresponding stable invariant manifold and at a certain point we perform a first velocity correction, say Δv_1. This is done to get to the neighbourhood of the Earth, in particular to reach a set of LEOs of fixed altitude h_{LEO} (LEO sphere). If this is the

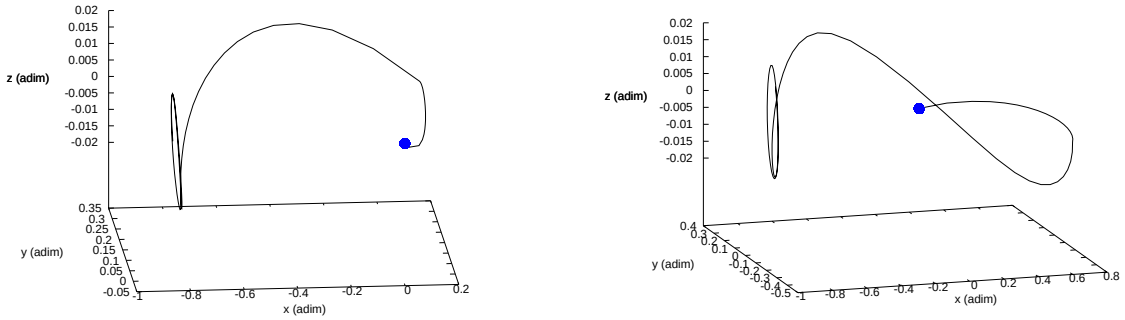

Figure 5: Examples of transfers obtained in the CR3BP synodical reference system. LEO of $h_{LEO} = 360$ km; arrival Lissajous orbit of amplitudes $\alpha_3 = \alpha_4 = 0.09$ normalized units (≈ 6000 km) around the L_1 point of the Earth – Moon system.

case, then another manoeuvre is required, Δv_2 defined as

$$\Delta v_2 = \sqrt{v^2 + v_c^2 - 2vv_c \cos(0.5\pi - \vartheta)}, \tag{10}$$

where $v_c = \sqrt{(1-\mu)/R}$ is the velocity on the LEO, $R = R_{Earth} + h_{LEO}$ ($R_{Earth} = 6378.14$ km), v is the velocity of the spacecraft arriving to the LEO backwards in time and ϑ is the angle between the normal to the LEO sphere and v.

As in the previous case, we do not want to take into account the time spent to wind up around the neighbourhood of the equilibrium point and hence we fix $t = 0$ when the component x fulfills a given requirement (generally $x > x_{min}$, where x_{min} is a well-defined value). Also, the initial conditions on the stable invariant manifold associated with the chosen Lissajous orbit are computed by means of an order 25 Lindstedt–Poincaré series expansion, taking $\alpha_1 = 0$, $\alpha_2 \neq 0$ and a certain number of values of ϕ_1 and ϕ_2 in the range $[0, 2\pi]$.

The main objective is to determine transfers as cheap as possible, that is, to look for the minimum $\Delta v_{tot} = \Delta v_1 + \Delta v_2$ which can guarantee the connection. In turn, this means to find Δv_1 such that Δv_2 is minimum or, equivalently, $\vartheta = 0.5\pi$, as stated by (10). We implement a differential correction procedure, having as initial seed a Hohmann-like transfer between the ellipse which osculates the point chosen on the manifold and a coplanar circular orbit with radius R around the Earth.

Recalling that a point on the hyperbolic manifold in synodical coordinates, say $(\mathbf{r}, \mathbf{v})$, can be seen as a point in sideral coordinates, say $(\mathbf{r}^{sid}, \mathbf{v}^{sid})$, within the Two – Body Problem framework, the objective is to satisfy

$$g := \mathbf{r}^{sid} \cdot \mathbf{v}^{sid} = \mathbf{v} \cdot \nabla G = 0, \tag{11}$$

where $G = (x-\mu)^2 + (y)^2 + (z)^2 - R^2$.

Concerning the results, the case of L_1 should be treated independently from the case of L_2, essentially due to the presence of the Moon in the latter case.

For orbits around the L_1 point, the negative branch of the stable invariant manifold associated with the nominal quasi-periodic orbit is the most suitable to our purpose. We take insertion points on the stable invariant manifold every $\Delta t = 0.01$ adimensional units (about 1 hour) up to $t = 9$ adimensional units (about 40 days), starting from 20×20 initial conditions along the Lissajous orbit. Two examples of the transfers computed are displayed in Fig. 5.

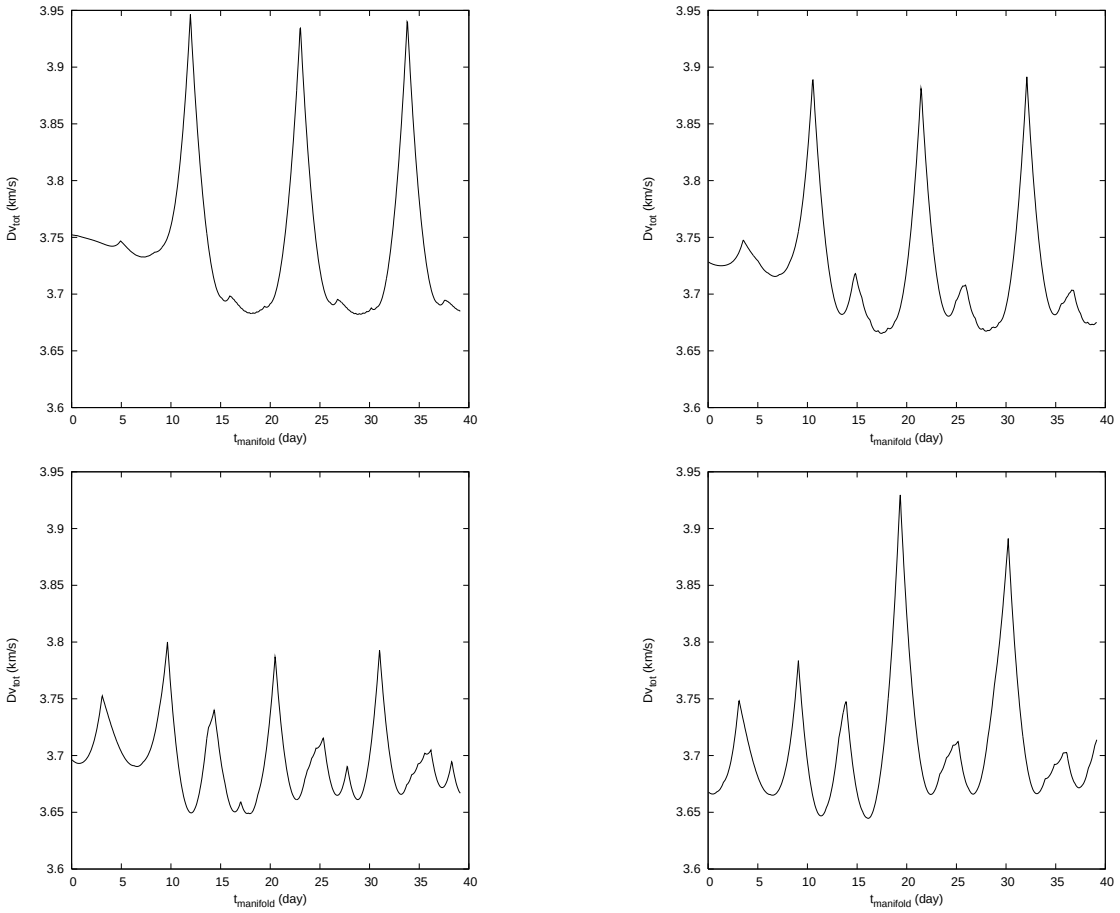

Figure 6: Minimum Δv_{tot} (km/s) found for each t (day) considered in the 20×20 mesh of points chosen. On the top left, L_1 Lissajous orbit of $\alpha_3 = 0.01$ normalized units (≈ 600 km); on the top right, $\alpha_3 = 0.03$ normalized units (≈ 1700 km); on the bottom left, $\alpha_3 = 0.06$ normalized units (≈ 3500 km); on the bottom right, $\alpha_3 = 0.09$ normalized units (≈ 6000 km).

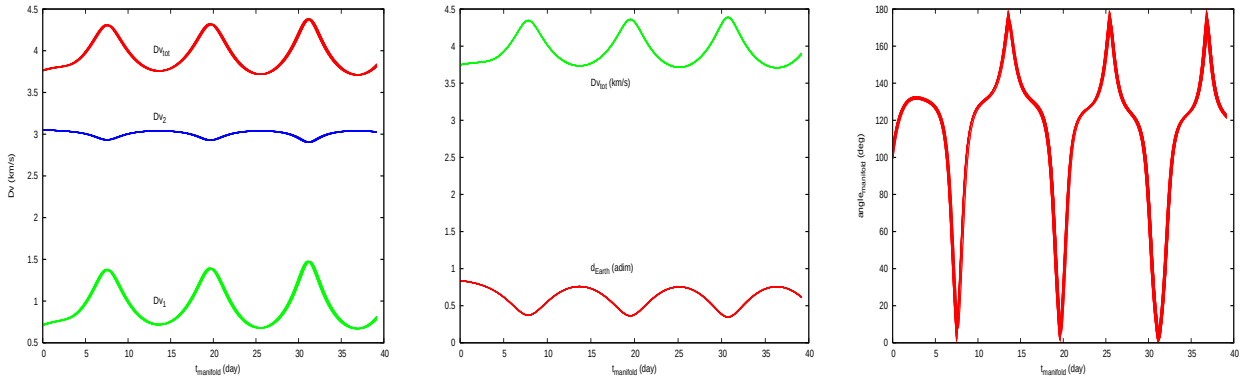

Figure 7: We display, as a function of the value of time corresponding to the insertion into the manifold, the behavior of Δv_1, Δv_2 and Δv_{tot} (left), of Δv_{tot} and d_{Earth} (middle) and of the angle between the velocity on the manifold and the velocity of insertion into the manifold (right).

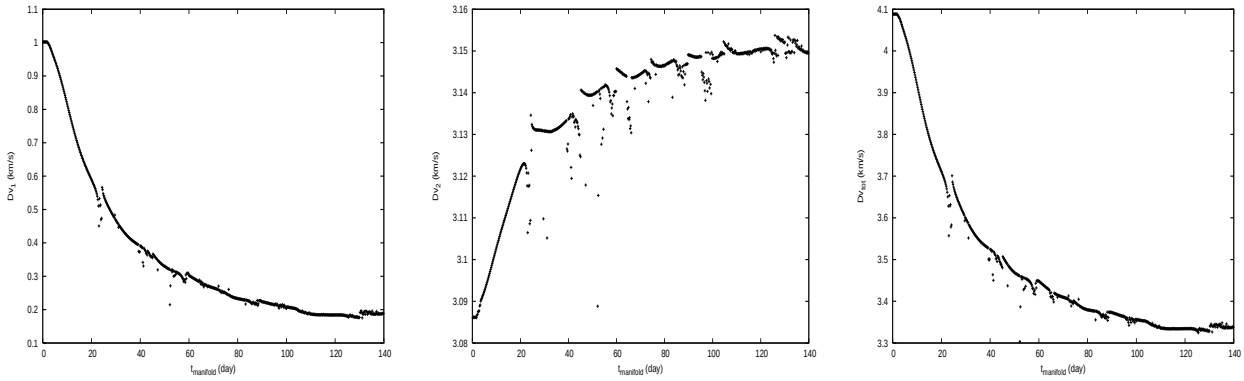

Figure 8: As a function of the time to be spent on the manifold, we plot Δv_1, Δv_2 and Δv_{tot} required to connect a LEO of $h_{LEO} = 360$ km and the positive branch of the stable invariant manifold associated with the L_2 square Lissajous orbit of amplitude $\alpha_3 = \alpha_4 = 0.12$ normalized units (≈ 10000 km) in the Earth – Moon system. Units day, km/s.

It turns out that the most expensive manoeuvre takes place on the LEO and that the greater the altitude h_{LEO} the smaller both manoeuvres Δv_1 and Δv_2, as expected. Also, the whole procedure allows to depart from LEOs at equatorial inclination. Going from the LEO to the manifold requires a time between 1 and 4 days. The greater the nominal Lissajous orbit, the cheaper and longer the transfer.

Analyzing the minimum Δv_{tot} obtained at each insertion point, we obtain plots as those showed in Fig. 6. The oscillations that appear in such curves are related to the distance d_{Earth} existing between the Earth and the point on the manifold corresponding to a given value of time. We notice that Δv_2, the manoeuvre on the LEO, is almost constant whenever we insert into the manifold, while Δv_1 is driven by the Earth–manifold distance. In particular, Δv_1 controls the conduct of Δv_{tot} and in turn, maxima of Δv_1 are associated with minima of d_{Earth}. These minima correspond to a change in velocity which lies on the opposite direction of the velocity associated with the point on the manifold. A maximum occurs when the change takes place in the same direction. See Fig. 7.

We can also achieve the transfer by inserting directly into the Lissajous orbit. In this case, Δv_1 is applied to the initial conditions given by the Lindstedt–Poincaré expansion setting $\alpha_1 = \alpha_2 = 0$. As it could also be deduced from Fig. 6, we cannot detect any improvement, apart from the total time of flight.

Regarding the L_2 point, as it stays beyond the Moon, there exist several manners in which our problem can be addressed, for instance by taking advantage of heteroclinic connections or lunar gravity assists. Here we analyze the efficiency of the methodology developed, for transfers joining a nominal LEO and the positive branch of the stable invariant manifold, which is the one moving away from the Earth – Moon neighbourhood. In this case, we discretize the whole branch at step of 1 hour up to 140 days.

The general behavior detected is showed in Fig. 8. As the time to be spent on the manifold increases, the cost of the two manoeuvres decreases, tending exponentially to a constant cost which depends on the value of h_{LEO}. This consideration holds whatever Lissajous amplitude we are considering. In the same figure, we can also notice that there exist some discontinuities. They are due to the Moon, which is encountered by some of the Hohmann-like legs constructed.

4 REFINEMENT OF ORBITS

The transfers described previously are computed under the approximation of the CR3BP. Though it provides results which work in several situations, it does not comprehend all the forces acting on a spacecraft.

The objective of this section is to present a robust algorithm which allows to refine a trajectory computed under the approximation of any simplified model to one satisfying more realistic equations of motion. To this end, we define a constrained optimization problem, the initial seed being a discretization in time of the trajectory computed with the reduced vectorfield.

In a nutshell, we aim at finding a trajectory which satisfies new equations of motion and verifies a local minimum of a given objective function, say F_{obj}, and some specific constraints. The main tool exploited is an optimizer. The main properties we ask to the procedure is to be versatile and modular.

The initial trajectory is splitted in $N-1$ sub-arcs, that is, in N nodes of the type

$$(t, \mathbf{X})_i \equiv (t_i, x_i, y_i, z_i, \dot{x}_i, \dot{y}_i, \dot{z}_i), \qquad (i = 1, \ldots, N).$$

We associate to each node a *departure* and *arrival* velocity, defined as

$$\mathbf{v}_i^A \;=\; \varphi(t_i; t_{i-1}, \mathbf{X}_{i-1})_{|\mathbf{v}}, , \qquad \mathbf{v}_i^D \;=\; (\dot{x}_i, \dot{y}_i, \dot{z}_i), \tag{12}$$

where $\varphi(t_i; t_{i-1}, \mathbf{X}_{i-1})$ is the flow at time t_i associated with the initial condition $(t_{i-1}, \mathbf{X}_{i-1})$ under the new vectorfield.

We want the optimizer to converge to N nodes such that:

- the objective function is at a local minimum in a given domain D:

$$F_{obj}(t_1, \ldots, t_N, \mathbf{X}_1, \ldots, \mathbf{X}_N) = \underset{(t,\mathbf{X})\in D}{min}\, F_{obj}(t, \mathbf{X}), \tag{13}$$

- the new trajectory is continuous in position:

$$\varphi(t_i; t_{i-1}, \mathbf{X}_{i-1})_{|\mathbf{r}} = (x_i, y_i, z_i), \qquad i = 2, \ldots, N, \tag{14}$$

- some constraints (in the domain of the variables, non-linear and linear) are fulfilled:

$$\mathbf{l} \leq \begin{pmatrix} (t, \mathbf{X})_i \\ \mathbf{c}(t, \mathbf{X})_i \\ A(t, \mathbf{X})_i \end{pmatrix} \leq \mathbf{u}. \qquad i = 1, \ldots, N, \tag{15}$$

  where $\mathbf{l}$ and $\mathbf{u}$ are lower and upper bounds set, respectively.

The last condition allows, in particular, to define boundary conditions.

So far we have taken advantage of SNOPT (Sparse Nonlinear OPTimizer) and IPOPT (Interior Point Optimizer), obtaining the best results with the last one. They both need the gradient of F_{obj} and the gradient associated with each constraint imposed. These gradients form the row of the Jacobian matrix used in the optimization algorithm.

We implement two definitions for F_{obj}, both of them accounting for the total Δv – cost along the path. In the first one, as F_{obj} we set the sum of the square of the manoeuvres required at each node, that is,

$$F_{obj} = \sum_{i=1}^{N} w_i ||\Delta \mathbf{v}_i||^2 = \sum_{i=1}^{N} w_i ||\mathbf{v}_i^A - \mathbf{v}_i^D||^2, \tag{16}$$

where w_i represents a weight associated with the node i. This is actually a very useful tool to control the manoeuvres to be done. For instance, a big w_i with respect to the other weights helps to obtain a smaller cost at the $i-$node.

The second one is more realistic, but it may bring numerical difficulties when the manoeuvres are very small:

$$F_{obj} = \sum_{i=1}^{N} w_i ||\mathbf{v}_i^A - \mathbf{v}_i^D||. \tag{17}$$

Note that the first and the last node are 'special' nodes, in the sense that we choose the velocity of arrival for the first node, v_1^A, and the velocity of departure for the last one, v_N^D. They can be specific functions and depend on all the variables of the problem.

To meet the continuity condition and to compute $\mathbf{v}_i^D$ and $\mathbf{v}_i^A$, we need to integrate from t_{i-1} to t_i, $(i = 2, \ldots, N)$. This is done by means of a *target* procedure. With this formulation, the velocity does not appear as a variable of the problem but it is computed with a Newton – Raphson method. More precisely, starting from the time t_{i-1} and position $\mathbf{r}_{i-1}$ associated with the node $i-1$, $(i = 1, \ldots, N-1)$ and a suitable initial guess, we look for the closest $\mathbf{v}_{i-1}^D$ which guarantees to reach $\mathbf{r}_i$ in an interval of time equal to $(t_i - t_{i-1})$. Once obtained convergence, we get $\mathbf{v}_{i-1}^D$ and also $\mathbf{v}_i^A$. We notice that in this way the optimization involves just (t_i, x_i, y_i, z_i) and thus the gradient of F_{obj} and of any constraint on the manoeuvres is not explicit.

The algorithm includes a set of regular constraints that can be imposed to each node. In particular, to not move the position of the $i-$node more than a certain amount with respect to the initial guess; to not move the time associated with the $i-$node more than a certain amount with respect to the initial guess; to bound the manoeuvre required at the $i-$node of a certain amount.

Apart from that, we incorporate some extra features. For instance, to transform between different reference systems, to compute orbital elements, to plot the trajectory at each iteration of the optimization, to add/remove nodes, to save information at each iteration of the optimization (e.g. F_{obj}).

In turn, we build a package that can be easily exploited. A general user should provide the initial guess for the trajectory, the new vectorfield and choose the constraints he needs among the ones available. He could add some additional ones, by providing the definition and the corresponding derivatives. There also exists the option to not load all the variables into the optimizer: for instance, in order to reduce the computational effort; to employ some nodes just in the target procedure, if parallel shooting is required; if we want to arrive to a given position at a well-defined epoch.

We are considering different applications for this tool. Until now, the tests have been performed on the refinement of Earth – Moon and Sun – Earth Lissajous orbits, of heteroclinic Earth – Moon and Sun – Earth connections and of the transfers described previously. They all have been refined considering as new vectorfield the Restricted N – Body Problem introduced at the beginning. Important ingredients to get convergence are represented by the accuracy of the initial guess, the values of the weights w_i and the extra constraints set.

As example, in Fig. 9, we show two LEO – L_1 Lissajous transfers refined, in the synodical and in the inertial coordinates. In Tab. 1, there are the corresponding cost of the manoeuvres computed with the two approximations. We cannot notice any remarkable distinction. The refinement is obtained by asking all the manoeuvres to be under a given tolerance, except for the ones at the LEO and at the insertion into the leg belonging to the stable invariant manifold. Moreover, we demand the first node to lay at an altitude of 360 km with respect to the surface of the Earth.

We recall that the constraints to set change from one type of orbit to the other. In the cases explored, we always get results very close to those given by the CR3BP approximation.

Table 1: Cost of the manoeuvres corresponding to the LEO – L_1 Lissajous transfers displayed in Fig. 9 under the CR3BP and the RNBP approximation.

I TRANSFER		
model	Δv_1 (km/s)	Δv_2 (km/s)
CR3BP	1.53	2.89
RNBP	1.51	2.91

II TRANSFER		
model	Δv_1 (km/s)	Δv_2 (km/s)
CR3BP	0.65	3.04
RNBP	0.66	3.05

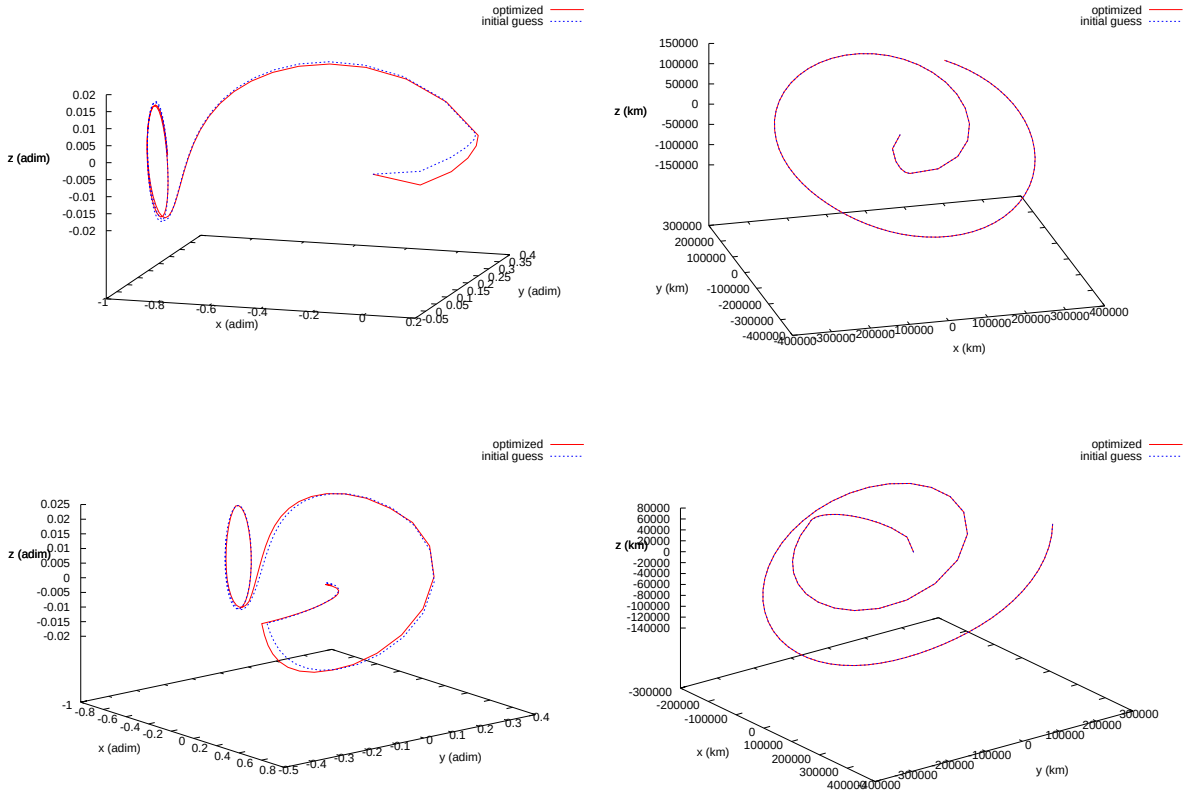

Figure 9: From the top, we show two LEO – L_1 Lissajous transfers refined to satisfy the RNBP equations of motion by means of our constrained optimization algorithm. Left: synodical coordinates; right: inertial one.

5 CONCLUSIONS

The dynamics corresponding to the stable manifold associated with the central manifold of the collinear equilibrium points L_1 and L_2 allows the design of rescue orbits from the surface of the Moon to a LPO and also of transfers from a nominal LEO to a LPO. In the second case, the connections are supported by two pieces, one of them not lying on the stable invariant manifold of the target orbit.

The target of the transfers are halo and Lissajous orbits of various sizes and the objectives of the work are achieved by means of semi-analytical and numerical techniques together with the usage of classical manoeuvres and the tools of Dynamical Systems Theory.

With respect to lunar rescue trajectories, in the direct case there are large regions on the Moon's surface from which the departure is not possible, independently of the nominal LPO selected. For non-direct orbits, which are characterized by a longer transfer time, rescue can take place from much larger regions.

Concerning the LPO – LEO transfers, if the nominal LPO is around the L_1 point the most advantageous connections take place when the fixed quasi-periodic orbit increases in size and at the maxima of the function distance between the Earth and the arrival point on the manifold we find the minima values for the total cost. This behavior can be explained in terms of the angle formed by the velocity on the manifold and the velocity of insertion on it. In the L_2 case, we get cheaper transfers than the L_1 ones, independently of the amplitude of the arrival orbit. The drawback is a long time of flight, which may not always be feasible from a practical point of view.

As showed in the second part of the work, the above trajectories can be refined assuming a more realistic model of forces, thanks to a constrained optimization technique. The cost of the manoeuvres and the shape of the trajectories obtained do not change meaningfully. In this sense, the Circular Restricted Three – Body Problem turns out to be a vey good framework to deal with.

Deepen discussions about LPO – LEO transfers and the constrained optimization approach will appear in forthcoming papers.

References

[1] Szebehely V., *Theory of orbits*, Academic Press, New York, 1967.

[2] Masdemont J.J., *High-order expansions of invariant manifolds of libration point orbits with applications to mission design*, Dynamical Systems: An International Journal, Vol. 20, 59–113, 2005.

[3] Richardson D.L., *A Note on Lagrangian Formulation for Motion About the Collinear Points*, Celestial Mechanics and Dynamical Astronomy, Vol. 22, 231–236, 1980.

[4] Gómez G., Jorba À, Masdemont J., Simó C., *Dynamics and Mission Design Near Libration Point Orbits – Volume* 3*: Advanced Methods for Collinear Points*, World Scientific, 2000.

[5] Alessi E.M., Gómez G., Masdemont J.J., *Leaving the Moon by means of invariant manifolds of libration point orbits*, Commununications in Nonlinear Science and Numerical Simulation, Vol. 14, 4153–4167, 2009.

[6] Rausch R.R, *Earth to Halo Orbit Transfer Trajectories*, Master of Science thesis, Purdue University, Indiana, 2005.

[7] Parker J.S., *Low–Energy Ballistic Lunar Transfers*, Ph.D thesis, University of Colorado, Boulder, Colorado, 2007.

[8] Renk F. and Hechler M., *Exploration Missions in the Sun – Earth – Moon system: A Detailed View on Selected Transfer Problems*, IAC-08-A5.3.5, 2008.